Fast Brillouin optical time domain analysis for dynamic sensing

Yair Peled,* Avi Motil, and Moshe Tur

The Faculty of Engineering, Tel-Aviv University, Tel-Aviv 69978, Israel
*yairpeled@gmail.com

Abstract: A new technique for the fast implementation of Brillouin Optical Time Domain Analysis (BOTDA) is proposed and demonstrated, carrying the classical BOTDA method to the dynamic sensing domain. By using a digital signal generator which enables fast switching among 100 scanning frequencies, we demonstrate a truly distributed and dynamic measurement of a 100m long fiber with a sampling rate of ~10kHz, limited only by the fiber length and the frequency granularity. With 10 averages the standard deviation of the measured strain was ~5 με.

OCIS codes: (060.2370) Fiber optic sensors; (290.5830) Brillouin scattering, (330.1880) detection; (190.0190) Nonlinear optics.

References and links

1. K. Y. Song, M. Kishi, Z. He, and K. Hotate, "High-repetition-rate distributed Brillouin sensor based on optical correlation-domain analysis with differential frequency modulation," Opt. Lett. **36**(11), 2062–2064 (2011).
2. A. Voskoboinik, J. Wang, B. Shamee, S. R. Nuccio, L. Zhang, M. Chitgarha, A. E. Willner, and M. Tur, "SBS-Based fiber optical sensing using frequency-domain simultaneous tone interrogation," J. Lightwave Technol. **29**(11), 1729–1735 (2011).
3. Y. Peled, A. Motil, L. Yaron, and M. Tur, "Slope-assisted fast distributed sensing in optical fibers with arbitrary Brillouin profile," Opt. Express **19**(21), 19845–19854 (2011).
4. Y. Peled, A. Motil, L. Yaron, and M. Tur, "Distributed and dynamical Brillouin sensing in optical fibers," Proc. SPIE **7753**, 775323, 775323-4 (2011).
5. Y. Peled, A. Motil, and M. Tur, "Fast microwave-photonics frequency sweeping for Brillouin ranging of strain or temperature," in *Proceedings of IEEE Conference on Microwaves, Communications, Antennas and Electronics Systems, (*IEEE, 2011).
6. M. Nikles, L. Thevenaz, and P. A. Robert, "Brillouin gain spectrum characterization in single-mode optical fibers," J. Lightwave Technol. **15**(10), 1842–1851 (1997).
7. K. Hotate, K. Abe, and K. Y. Song, "Suppression of signal fluctuation in Brillouin optical correlation domain analysis system using polarization diversity scheme," IEEE Photon. Technol. Lett. **18**(24), 2653–2655 (2006).
8. A. W. Brown, B. G. Colpitts, and K. Brown, "Dark-pulse Brillouin optical time-domain sensor with 20-mm spatial resolution," J. Lightwave Technol. **25**(1), 381–386 (2007).
9. W. Li, X. Bao, Y. Li, and L. Chen, "Differential pulse-width pair BOTDA for high spatial resolution sensing," Opt. Express **16**(26), 21616–21625 (2008).
10. S. M. Foaleng, M. Tur, J. C. Beugnot, and L. Thevenaz, "High spatial and spectral resolution long-range sensing using brillouin echoes," J. Lightwave Technol. **28**(20), 2993–3003 (2010).

1. Introduction

The widely used Brillouin Optical time Domain Analysis (BOTDA) technique is based on stimulated Brillouin scattering (SBS), where two counter-propagating light waves, most often a pulsed pump and a CW probe, interact along a sensing fiber. At each point in time, the probe wave at a specific location may be amplified by the traveling pump pulse, depending on the frequency difference between these two light waves. By scanning the optical frequency of either wave with respect to the other, the narrow (30MHz) Brillouin Gain Spectrum (BGS) is recovered, and the frequency difference, gauged by the location of the peak gain, can be translated to strain or temperature at each point along the sensing fiber. Although a very useful technique, its currently common implementations are relatively slow, on the orders of seconds to minutes. Recently, a technique based on Brillouin Optical Correlation Domain Analysis (BOCDA), has experimentally achieved the true distributed measurement of a 1.3Hz fiber vibration, acquired at a repetition rate of 20Hz at a spatial resolution of 80cm over a

#162416 - $15.00 USD Received 2 Feb 2012; revised 2 Mar 2012; accepted 2 Mar 2012; published 28 Mar 2012

100m fiber [1]. A different approach proposes to use multiple pumps and multiple probes to avoid the time-consuming frequency sweeping time required by the classical BOTDA technique. Measurement speed will potentially increase but at the expense of frequency granularity [2]. A recently demonstrated BOTDA based method, called Slope Assisted (SA) BOTDA, probes the fiber with a single frequency, located at the middle of the slope of the local BGS, allowing a single pump pulse to sample fast strain variations along the full length of the fiber [3, 4]. By using a specially synthesized and adaptable probe wave, a fiber with an arbitrary distribution of the Brillouin frequency shift (BFS) can be interrogated. Strain vibrations of up to 400Hz were demonstrated, simultaneously measured on two different sections of an 85m long fiber, having different static Brillouin shifts and with a spatial resolution of 1.5m. Although fully distributed and very fast, the measured strain vibration amplitude is limited to the extent of the linear section of the BGS slope (~600 με @ a 10ns pump pulse).

Four main factors control the sensing speed of a BOTDA setup [5]:

1) Time of Flight: the repetition rate of the pump pulses should not exceed $1/T_{round\_trip}\ (=2L/V_g)$, where V_g is the group velocity speed of light traveling inside the fiber and L is the fiber's length.

2) Averaging over N_{avg} (= 10 to thousands) pump pulses is required to achieve satisfactory signal to noise ratio (*SNR*), especially over long fibers.

3) Scanning granularity: in order to precisely map the Brillouin gain within the expected dynamic range of strain/temperature variations, N_{freq} = 100 to 200 different frequencies should be probed.

4) Optical frequency switching speed of the sweep mechanism requires a finite time, depending on the actual implementations: on the order of milliseconds or longer, inclusive of stabilization.

The first length dependent factor cannot be improved. The second solely depends on the available *SNR* from a single pump pulse, which in turn, depends on system design and nonlinear effects in the fiber under test (FUT). The third factor is determined by the required strain/temperature resolution. The first two factors are dominant for long (tens of kilometers) sensing fibers, resulting in long acquisition times on the order of minutes. On the other hand, when dealing with a relatively short (less than 1km) fiber, the fourth factor, frequency switching speed, becomes dominant. The technique proposed and demonstrated in this paper enables almost an instantaneous frequency transition (on the order of nanoseconds). Furthermore, when dealing with a short sensing fiber, a stronger pump pulse can be launched into the fiber without giving rise to undesired nonlinear effects, enabling a much better *SNR* (per a single pump pulse), so that much fewer averages are required, thereby reducing the weight of the second factor. Thus, if we ignore the frequency switching time, the time required for a complete scan of the BGS, including N_{avg} averages and M_{freq} frequency steps, is given by:

$$T_{scan} = N_{avg} N_{freq} T_{round\_trip} \tag{1}$$

In this work we demonstrate one complete distributed (1.3m spatial resolution) Brillouin scan of a 100m long fiber using 100 optical frequencies in 120 microseconds. With 10 averages (i.e., in 1.2ms), a BGS was reconstructed with a BFS standard error of less than 0.25MHz.

2. Method

Here we use the well-known approach [6] to generate both the pump and probe waves from the same highly coherent laser by using an electro-optic modulator to create a frequency

#162416 - $15.00 USD Received 2 Feb 2012; revised 2 Mar 2012; accepted 2 Mar 2012; published 28 Mar 2012

difference between the pump (directly derived from the laser) and probe (down shifted in frequency from that of the laser by a controllable difference on the order of the BFS~11GHz). The modulator is normally driven by a relatively slowly sweeping YIG- or VCO-based electronic synthesizer, whose frequency is scanned at a rate on the order of 1ms per frequency step (or slower), to cover the frequency span of interest (100's of MHz). Instead, we propose the use of an arbitrary waveform generator (AWG). While the pump pulse frequency is maintained at a fixed value, the probe frequency can be changed every $T_{round\_trip} = 1\mu s$ (for a 100m long fiber). This very fast change is obtained by first writing into the deep memory of the AWG a numerical description of 1μs long sine wave of the first frequency, followed by the numerical description of 1μs long sine wave of the second frequency, until all N_{freq} frequencies have been recorded. Then, in synchronization with the first pump pulse, the digital to analog output stage of the AWG emits a 1μs long analog sine wave of the first frequency, followed by a 1μs long analog sine wave of the second frequency, destined to meet the second pump pulse, and so on and so forth until the last frequency has been launched. This sequence of N_{freq} scans defines a temporal frame of length $T_{frame} = N_{freq} T_{round\_trip}$, Fig. 1(a). For averaging and *SNR* improvement, the process repeats itself for N_{avg} times. Clearly, the same fast scanning idea can be equally implemented by keeping a fixed probe frequency while fast changing the frequency of the pump pulse, Fig. 1(b). In either case, one could perform the N_{avg} averages per frequency before switching to the next frequency. Clearly, this mode is less demanding on the frequency switching speed but compromises the sampling rate of the phenomenon to be sensed. Additionally, the first type of data acquisition allows a more flexible post-processing, e.g., performing different amounts of averaging on different fiber segments.

The main characteristics required from the AWG are: (*i*) wide bandwidth of at least a few hundred MHz to be able to cope with the dynamic range spanned by the varying strain and temperature along the fiber; and (*ii*) deep enough memory to contain all waveforms representing the planned scan frequencies. While these two requirements are met in full by a few currently available AWGs, it is very difficult to find an AWG which can directly synthesize frequencies around the required center frequency of ~11GHz. Instead, as shown in Sec. 3, frequency upconversion can lift the output of ~1GHz AWGs to the Brillouin regime. We call this variant of BOTDA: Fast BOTDA, or F-BOTDA for short.

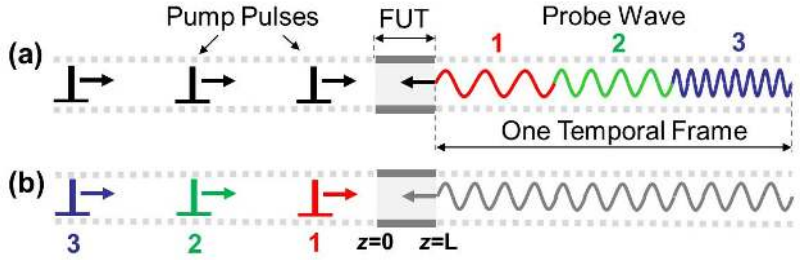

Fig. 1. An example of F-BOTDA fast sweep assembled from three frequencies. Normally, such a sweep comprises between 100 and 200 different frequencies. (a) A sequence of fixed frequency pump pulses meet probe waves of different frequencies. (b) The probe frequency is fixed while the frequency of the pump pulse changes from one pulse to the other.

Finally, it should be noted that a lot of data is involved in fast repeated acquisition of the full Brillouin distance-frequency map. One method to collect, process and present the measured data of F-BOTDA will be discussed in the following section.

#162416 - $15.00 USD Received 2 Feb 2012; revised 2 Mar 2012; accepted 2 Mar 2012; published 28 Mar 2012

3. Experiment

A highly coherent 1550nm DFB laser diode (DFB-LD), with a linewidth of 10kHz, is split into pump and probe channels, Fig. 2. A complex waveform, of the shape of Fig. 1, to be described in more details below, feeds the probe channel Mach-Zehnder modulator (EOM1), which is biased at its zero transmission point to generate two sidebands, the lower one for the probe wave and the upper one to be discarded later by the fiber Bragg grating (FBG) filter. The EOM1 output is then amplified by an Erbium doped fiber amplifier (EDFA1), optionally scrambled by a polarization scrambler (PS), and launched into one side of the fiber under test (FUT), Fig. 3, through an attenuator (ATT). Modulator EOM2 forms a 13ns pump pulse, which is amplified by EDFA2 and launched into the other side of the FUT through a circulator (CIR1). The Brillouin-amplified probe wave is finally routed to a fast photodiode (PD) by CIR1 and CIR2. A narrow bandwidth fiber Bragg grating (FBG) filters out pump backscattering, as well as the upper sideband generated by EOM1. Finally, the output of the photodiode is sampled at $f_{samp} = 1$ GSamples/s by a real-time oscilloscope with deep memory.

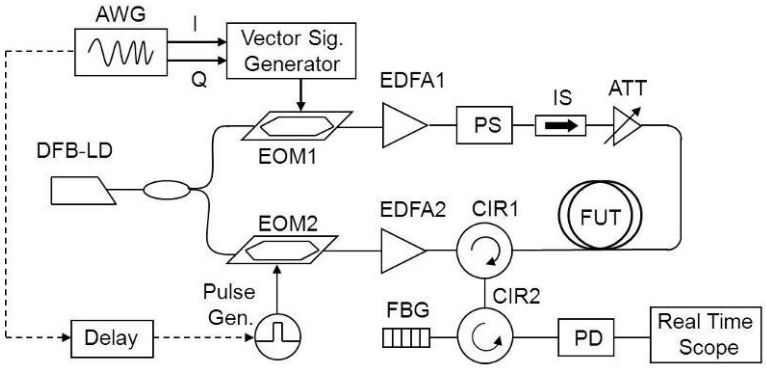

Fig. 2. Experimental setup: AWG: arbitrary waveform generator, EOM: electro-optic modulator, EDFA: Erbium-doped fiber amplifier, CIR: circulator, FBG: fiber Bragg grating, PS: polarization scrambler, IS: isolator, ATT: attenuator, FUT: fiber under test, PD: photodiode.

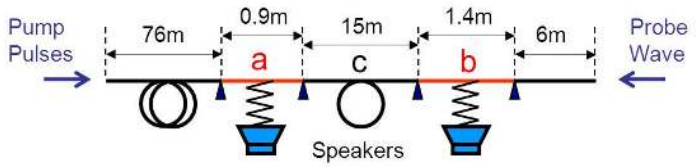

Fig. 3. The 100m FUT comprising five sections of SMF fiber. The two sections of 0.9m (a) and 1.4m (b) are mounted on manually stretching stages, making it possible to adjust their static Brillouin frequency shifts. Additionally, audio speakers are physically attached to these two sections in order to induce fast strain variations of various frequencies and magnitudes. Segment **c** is loosed as the rest of the fiber.

Obtained from the lower sideband of the modulator output, the optical frequency of the probe signal is given by $v_{probe} = v_{laser} - f = v_{pump} - f$, where f is the frequency of the RF signal at the modulator input. In standard single mode fibers at 1550nm, the BFS is around 11GHz and quite a wide range of temperature and strain variations can be monitored by scanning the frequency f over a range of a few hundred MHz around 11GHz with a specified granularity. Our method calls for an essentially instantaneous switching of the scanning frequency, a task which cannot be currently performed by commercial frequency synthesizers. The required fast switching (~1ns) can be achieved by high-speed arbitrary

#162416 - $15.00 USD Received 2 Feb 2012; revised 2 Mar 2012; accepted 2 Mar 2012; published 28 Mar 2012

waveform generators (AWGs), most of which are still limited to a few GHz. In this experiment we used a combination of a dual-channel 500MHz AWG together with a microwave vector signal generator with I/Q inputs to achieve a clean RF modulating signal, having a fast changing frequency, covering up to 1GHz around 11GHz.

To generate a sequence of signals of frequencies: $\left\{ f_i = f_{start} + (i-1) f_{step},\ i = 1 \ldots N_{freq} \right\}$, the microwave signal generator frequency, f_c, was set to a fixed value around 11GHz and the two channels of the AWG, $V_I(t)$ and $V_Q(t)$ were programmed to synthesize cosine and sine waveforms at baseband frequencies $\left\{ (f_i - f_c),\ i = 1 \ldots N_{freq} \right\}$:

$$\begin{aligned} V_I(t) &= V_0 \sum_{i=1}^{N_{freq}} \mathrm{rect}\left(\frac{t}{T_{round\_trip}} + \frac{1}{2} - i \right) \cos\left[2\pi (f_i - f_c) t \right]; \\ V_Q(t) &= V_0 \sum_{i=1}^{N_{freq}} \mathrm{rect}\left(\frac{t}{T_{round\_trip}} + \frac{1}{2} - i \right) \sin\left[2\pi (f_i - f_c) t \right]; \end{aligned} \tag{2}$$

A frequency synthesizer with I/Q modulation capabilities mixes its I ($V_I(t)$) and Q ($V_Q(t)$) inputs with a high frequency carrier, generated by the synthesizer at frequency f_c, to produce a clean RF output of the required form:

$$\begin{aligned} V_{RF}(t) &= V_I(t)\cos(2\pi f_c t) - V_Q(t)\sin(2\pi f_c t) \\ &= V_0 \sum_{i=1}^{N_{freq}} \mathrm{rect}\left(\frac{t}{T_{round\_trip}} + \frac{1}{2} - i \right) \cdot \left[\cos[2\pi (f_i - f_c) t]\cos(2\pi f_c t) - \sin[2\pi (f_i - f_c) t]\sin(2\pi f_c t) \right] \\ &= V_0 \sum_{i=1}^{N_{freq}} \mathrm{rect}\left(\frac{t}{T_{round\_trip}} + \frac{1}{2} - i \right) \cos\left[2\pi \left(f_{start} + (i-1) f_{step} \right) t \right] \end{aligned} \tag{3}$$

Ideally, this RF signal instantaneously switches between consecutive frequencies. In practice the switching speed is limited by the analog bandwidth of the AWG to less than 1ns. Unlike a simple RF mixer, the I/Q modulator highly suppresses the carrier and unwanted images.

In this experiment the probe wave optical frequency was swept between f_{start} = 10.8GHz and f_{end} = 10.998GHz below that of the optical frequency of the pump, in N_{freq} = 100 frequency steps of f_{step} = 2MHz, the duration of which should be at least T_{round_trip} long. Due to the technical specifications of the AWG, the duration of each frequency was set to1.2μs (instead of 1μs for the 100m FUT), which is long enough for a single pump pulse to interrogate a 120m long fiber. Using T = 1.2μs and N_{freq} = 100 leads to $T_{temporal\_frame} = 120\mu s$. Thus, the acquisition rate was ~8.3kHz, enabling the measurement of vibrations as fast as 4kHz. Polarization considerations may slow this fast sampling rate. Indeed, to mitigate the dependence of the Brillouin gain on the fiber birefringence, some kind of polarization scrambling must be invoked. Switching the pump or probe polarization between two orthogonal states [7] will reduce the sampling speed by half. Random scrambling can also be applied with minimum impact if averaging is used to improve the *SNR* of the Brillouin signal. The reported measurements were taken without a polarization scrambler. Instead, the polarization of the probe wave was adjusted by a polarization controller (PC) so that both stretched sections (**a** and **b** in Fig. 3) experienced the same Brillouin gain.

The measurement ended with one long vector of 50 million samples, taken over 50ms. For analysis, the sampled vector was segmented into shorter vectors of length $N_{cycle} = T_{round\_trip} \cdot f_{samp} (= 1200)$, and then to groups of N_{freq} short vectors each, which could then be stored as an $N_{cycle} \times N_{freq}$ (1200X100) array. Each array, to be referred to later as a temporal frame, holds a complete distance-frequency map of the distributed BGS measurement of the fiber over N_{freq} frequencies and N_{cycle} spatial points. For a measurement

#162416 - $15.00 USD Received 2 Feb 2012; revised 2 Mar 2012; accepted 2 Mar 2012; published 28 Mar 2012

carried out along an interval of $T_{measure}$ seconds, $N_{frame} = T_{measure} / (N_{freq} \cdot T_{round\_trip})$ such temporal frames can be assembled into a three dimensional (distance, frequency, time) matrix, $\mathbf{M}(N_{cycle}, N_{freq}, N_{frame})$, which contains the time evolution of the BGS of every spatial point along the fiber. A moving average of order N_{avg} along the N_{frame} axis of $\mathbf{M}$ can now be used to improve the signal to noise ratio and to accommodate random polarization scrambling.

4. Results

Figure 4 shows the last 20m of the 100m FUT of Fig. 3, having the two sections of length 90cm (**a**) and 140cm (**b**) statically stretched to the same strain (~800με), corresponding to a BFS of 40MHz higher than that of the loose fiber. Ten sequential temporal frames were averaged ($N_{avg} = 10, T_{scan} = 1.2$ms) to produce the figure. No further processing was applied. The observed spatial resolution (~1m) is that expected from the 13ns pump pulse. Then, segments **a** and **b** were vibrated at 100Hz and 80Hz, respectively, using the physically attached audio speakers. An in-between, non-vibrating fixed segment (**c**) was chosen as a static reference. With a pump pulse repetition rate of 833kHz, a continuous measurement of the Brillouin signal was taken at a sampling rate of 1GHz for 50ms, resulting in a 50M samples vector. With 100 scanning frequencies, the $T_{temporal\_frame}$ was 120μs long, representing an effective vibrations sampling rate of 8.33kHz. As described above, the data were arranged in the matrix $\mathbf{M}(N_{cycle}, N_{freq}, N_{frame})$, whose three dimensions, respectively represent, distance, frequency and time evolution.

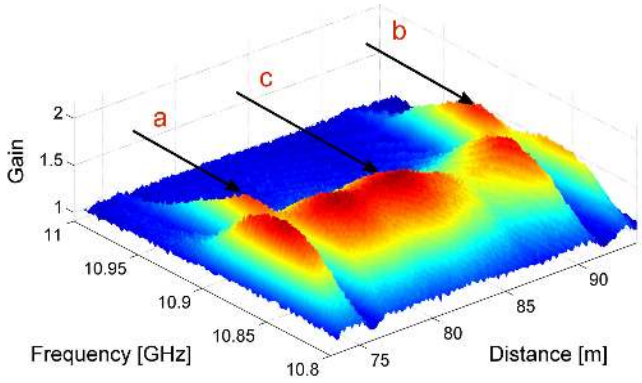

Fig. 4. A zoom in on the last 20m of the 100m fiber, having two sections of 90cm and 140cm long stretched to a static strain of ~800με. The interrogation of the whole 100m fiber took 1.2ms, including 10 averages.

When averaging was required, N_{avg} sequential temporal frames were averaged, effectively reducing the vibrations sampling rate by N_{avg} (833Hz for $N_{avg} = 10$). Slicing $\mathbf{M}(\cdot)$ at a certain distance z_1 (i.e., along its first dimension, N_{cycle}) gives a 2D, frequency-time matrix, which describes the time evolution of the BGS of the spatial resolution cell z_1. Figure 5 shows 3 different such slices along the FUT at $z = z_a$, $z = z_b$ and $z = z_c$. The vibrating dynamic strains, at 100Hz and 80Hz are clearly observed at segments **a** and **b**, while the BGS of segment **c** remains static. Quantitative analysis of the raw data of Fig. 5 was performed by fitting a Lorentzian curve to the measured BGS of each time slot.

#162416 - $15.00 USD Received 2 Feb 2012; revised 2 Mar 2012; accepted 2 Mar 2012; published 28 Mar 2012

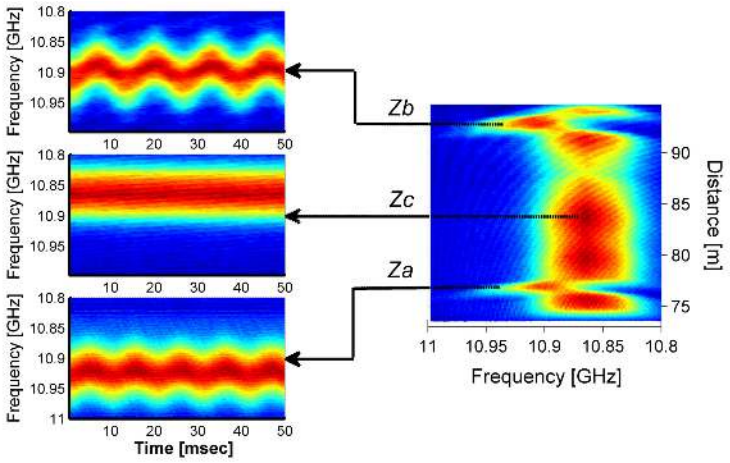

Fig. 5. On the right: Top view of Fig. 4, indicating the locations of the vibrating (**a** and **b**) and non-vibrating (**c**) segments of the FUT. On the left: the measured frequency distribution of the BGS as a function of time at three different segments of the FUT ($z = z_a$, $z = z_b$ and $z = z_c$). $N_{avg} = 10$. Vibrations of 100Hz and 80Hz are clearly observed at segments **a** and **b**, while segment **c** is static.

The calculated BGSs peaks, describing the time dependent BFS at segments **a** and **b,** are shown in Fig. 6. A movie, assembled from part of matrix $\mathbf{M}(\cdot)$, zooming on the three sections of interest can be viewed at Fig. 7 (Media 1).

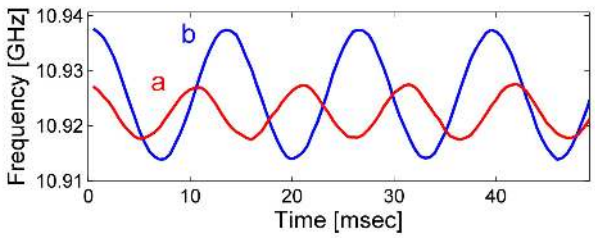

Fig. 6. The time dependent BFS of the two vibrating segments, as determined from the peaks of Lorentzian fits to the BGSs of each time slot.

The measurement frequency noise was evaluated by determining the standard deviation (*std*) of the BFS (after 10 averages and a Lorentzian fit) at the static segment **c**, and found to be as low as 0.25MHz (equivalent to ~5 με).

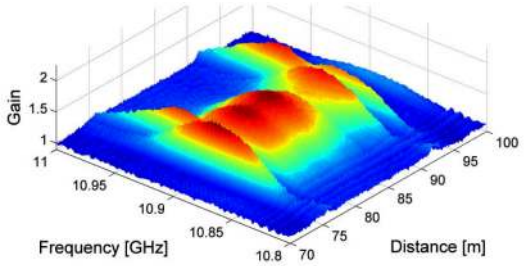

Fig. 7. Single-frame excerpts from a video assembled from matrix M, zooming on the last 20m of the FUT. Vibrations of segments **a** and **b** are observed (Media 1).

#162416 - $15.00 USD Received 2 Feb 2012; revised 2 Mar 2012; accepted 2 Mar 2012; published 28 Mar 2012

While the *full* contents of the $\mathbf{M}(\cdot)$ matrix is required for the F-BOTDA technique, a different cut through the matrix provides information on the time dependence of the Brillouin gain along the entire fiber at *one selected frequency*. Specifically, choosing this frequency to be at the middle of the slope of the time-averaged, Fig. 8(a), we obtain, Fig. 8(b), a Slope-Assisted BOTDA [3] measurement of both segments **a** and **b**, as well as the 15m non-vibrating in-between segment. Needless to say, this SA-BOTDA measurement, requiring only one frequency (f_{3dB}) could have been obtained in only $1/N_{freq}$ of the time required for the F-BOTDA technique, although only one gain point is measured.

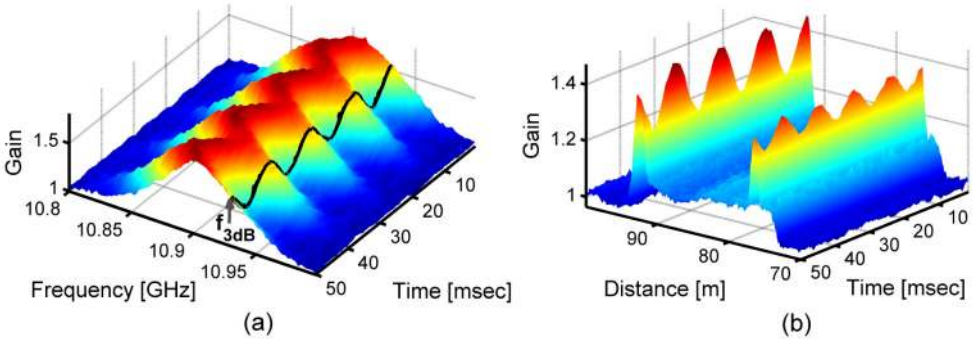

Fig. 8. (a) A 2D cut through the 3D $\mathbf{M}(\cdot)$ matrix at $z = z_b$, describing the measured BGS of segment **b** 80Hz vibrations as a function of time. The black line is an additional cut through the plotted 2D at frequency $f = f_{3dB}$ = 10.93GHz, showing the Brillouin gain variations as a function of time, at $z = z_b$ at a frequency located at the middle of the BGS slope. Thus, if one cuts the 3D matrix at $f = f_{3dB}$, a full Distance-Time Gain picture for the whole fiber is obtained from a single frequency probing. (b) A 2D cut from the 3D $\mathbf{M}(\cdot)$ matrix at $f = f_{3dB}$, describing the Brillouin gain as a function of time at the frequency f_{3dB} along the entire FUT. f_{3dB} designates the frequency at the middle of the slope of the averaged BGS. This technique is called SA-BOTDA [3].

5. Discussion and summary

We have proposed and demonstrated a new technique, F-BOTDA, for a very fast implementation of BOTDA, whose speed is basically limited only by the fiber length and the number of required averages. Fast switching of the optical frequency was achieved using an electronic arbitrary waveform generator, although it could be equally accomplished by customized and much cheaper electronics. This technique carries the classical BOTDA method from the static domain to the dynamic one. The proposed technique is useful mainly for short fiber sensors, on the order of a few hundred meters or less. As the fiber gets longer, it is the need for longer averaging, which starts to limit the acquisition rate. This F-BOTDA method was demonstrated on a 100m long fiber, having two vibrating segments of 90cm and 140cm towards its end. Full scans of the BGS, using 100 frequencies, were done at a rate of 8.3kHz, easily capturing the 80Hz and 100Hz induced vibrations. With only ten averages, a fairly low standard deviation of 0.25MHz was obtained, corresponding to ~5 με. Since this technique is based on classical BOTDA, most BOTDA recently introduced methods for high spatial resolution [8–10], can be employed to achieve fast dynamical and distributed Brillouin sensing with high spatial resolution. Finally, although real time implementations of the technique would involve the recording and processing of large amount of data, modern data acquisition and signal processing circuitry can handle the challenge at a post averaging sampling rate of hundreds of hertz.

#162416 - $15.00 USD Received 2 Feb 2012; revised 2 Mar 2012; accepted 2 Mar 2012; published 28 Mar 2012